Available online at www.sciencedirect.com
SCIENCE DIRECT®
Journal of Sound and Vibration 275 (2004) 577–590
JOURNAL OF SOUND AND VIBRATION
www.elsevier.com/locate/jsvi

Damage identification in structures using the time-domain response

S. Choi[a,*], N. Stubbs[b]

[a] *Structural Systems and Site Evaluation Department, Korea Institute of Nuclear Safety, Yoosung PO Box 114, Daejeon 305-600, South Korea*
[b] *Department of Civil Engineering, Texas A&M University, College Station, TX 77843, USA*

Received 19 August 2002; accepted 26 June 2003

Abstract

A methodology to locate and size damage in a structure using the time-domain response is presented in this paper. The measured response in the time domain is spatially expanded over the structure and the mean strain energy for a specified time interval is obtained for each element of the structure. The mean strain energy for each element is, in turn, used to build a damage index that represents the ratio of the stiffness parameter of the pre-damaged to the post-damaged structure. The damage indices are used to identify possible locations and corresponding severities of damage in the structure. The validity of the methodology is demonstrated using data from a numerical example of a beam structure.

1. Introduction

As concerns about the soundness of the civil engineering structures grow, the need to develop effective and practical structural health monitoring (SHM) systems is emerging as a prominent problem in structural engineering. SHM system includes a synthesis of experimental data gathering techniques and non-destructive damage evaluation (NDE) schemes. To date, numerous NDE methods have been proposed. The theoretical bases of these methods include neural networks [1], pattern recognition [2], sensitivity analysis [3,4], fuzzy sets [5], and system identification [6,7]. Recently, methods that attempt to simultaneously assess the condition of the whole structure, the so-called global NDE methods, have been gaining acceptance in

*Corresponding author. Tel.: +82-42-868-0666; fax: +82-42-868-0523.
E-mail addresses: schoi@kins.re.kr (S. Choi), n-stubbs@tamu.edu (N. Stubbs).

0022-460X/$ - see front matter © 2003 Elsevier Ltd. All rights reserved.
doi:10.1016/j.jsv.2003.06.010

the engineering community. The basic idea behind these global methods is that changes in the physical properties of a system alter the response characteristics of the structure. A recent round robin study involving five established NDE methods reveals that the damage index method [8] performed best using simulated data and data from a real structure [9].

The damage index method originated from a sensitivity approach that relates changes in modal responses, specifically resonant frequencies, to changes in the mass, damping, and stiffness of a structure. Based on work done by Cawley and Adams [10], Stubbs [11], and Stubbs and Rials [12] proposed a method that relates changes in the resonant frequencies to changes in element stiffness. To reduce the computational effort involved in the proposed scheme, Stubbs [13] developed an NDE theory using linear inverse method. Stubbs and Osegueda [3,4] further developed the method for applications to beams and other structures. To overcome the difficulties of the previous works, which arise when the number of vibrational modes is much less than the number of damage parameters to be determined, Stubbs et al. [8] developed the so-called damage index method. This method has been corroborated using (1) numerically simulated data for various structural types and classes [14,15], (2) experimental modal data generated in a laboratory environment [16], and (3) field data measured on bridge structures [9,17].

In recent years, most global NDE methods, including the damage index method, utilize modal data (i.e., resonant frequencies and modeshapes) to predict possible damage locations and estimate the severity of the damage. The modal data can be extracted using established experimental modal analysis techniques (input–output methods or output only methods) to estimate the modal parameters (i.e., resonant frequencies, modal damping, and mode shapes) [18]. However, the input–output modal parameter extraction method involves averaging and curve-fitting procedures which introduce additional uncertainties and measurement errors. Furthermore output-only extraction methods are computationally intensive. One potential solution to this problem is to investigate other types of response measures (e.g., static response [19], time-domain response [20], etc.) that circumvent these difficulties.

The objective of this paper is to develop a time-domain-based NDE methodology that obviates the computational demands, complexity, and subjectivity associated with current modal parameter extraction methods. In the proposed method, a mean strain energy measure which uses response data for a specified time period is utilized to formulate a damage index for an element in a structure. The damage indices, which represent the ratio of pre- and post-damaged stiffness of the elements, are utilized to identify the locations and corresponding severities of the possible damage locations. The validity of the methodology is demonstrated using numerically generated data from a continuous beam structure.

2. Theory

2.1. New damage ratio using the time-domain response

Suppose that dynamic responses of a structure are sampled at n locations at time interval Δt from $t_i = t_1$ to $t_i = t_{NT}$, where NT is the number of sampling points. Then, the sampled dynamic

responses for the n sensor locations may be expressed in matrix form as follows:

$$\begin{array}{l} \textit{Locations} \rightarrow \quad 1 \qquad\qquad j \qquad\qquad n \quad \textit{Time Step} \\ \qquad\qquad\qquad\qquad\qquad\qquad\qquad\qquad\quad \downarrow \\ W = \begin{bmatrix} w_{1,1} & \cdots & w_{1,j} & \cdots & w_{1,n} \\ \vdots & \ddots & \vdots & \iddots & \vdots \\ w_{i,1} & \cdots & w_{i,j} & \cdots & w_{i,n} \\ \vdots & \iddots & \vdots & \ddots & \vdots \\ w_{NT,1} & \cdots & w_{NT,j} & \cdots & w_{NT,n} \end{bmatrix} \begin{array}{l} 1 \\ \\ i \\ \\ NT \end{array} \end{array} . \tag{1}$$

In the matrix, the jth column vector represents dynamic displacements at the jth location, and the ith row vector represents the dynamic displacements at the ith time step. Using current technology, the discretized displacements can be obtained by integrating the acceleration records obtained from accelerometers [21]. Thus, each row vector describes the instantaneous deformed configuration of the structure at a certain instant of time. Consequently, there are NT response measurement sets, if a single row vector is regarded as one measurement set.

Since damage in a structure causes changes in the dynamic characteristics of the system such as frequencies and mode shapes, the displacement configurations of the pre-damaged and the post-damaged structures at the same sampling time will be different. Thus, the deformed configuration of the pre-damaged structure measured at a certain time should not be compared to the deformed configuration of the post-damaged structure at the same time. To overcome this difficulty, the mean strain energy of the structure over a sampling period is used here instead of the direct comparison between strain energies of pre- and post-damaged structures at the same time. The matrix expression presented in Eq. (1) may be rewritten as

$$W = [V_1, \ldots, V_i, \ldots, V_{NT}]^{\mathrm{T}}, \tag{2}$$

where a vector, V_i $(= V(t_i))$, represents a displacement configuration of the structure at time t_i. Considering a system with NE elements, the corresponding strain energy of the structure at a time t_i can be expressed as

$${}_sU_i = \tfrac{1}{2} V_i^{\mathrm{T}} K V_i, \tag{3}$$

where the subscript s refers to the structure. The mean strain energy for a specified time interval between t_a and t_b $(b > a)$, ${}_s\bar{U}_{\bar{i}}$, may be defined as

$${}_s\bar{U}_{\bar{i}} = E[{}_sU_i] = \frac{1}{2(b-a)} \sum_{i=a}^{b} V_i^{\mathrm{T}} K V_i. \tag{4}$$

Similarly, the average mean strain energy for the jth element in a structure may be given by

$${}_j\bar{U}_{\bar{i}} = E[{}_jU_i] = \frac{1}{2(b-a)} \sum_{i=a}^{b} V_i^{\mathrm{T}} K_j V_i, \tag{5}$$

where $K_j = k_j C_j$, k_j is the stiffness of element j, and C_j is the geometric portion of the contribution of the jth element to the system stiffness matrix. The ratio of the mean strain energy

for the jth element to the system mean strain energy is given by

$$F_j = \frac{{}_j\bar{U}_{\bar{i}}}{{}_s\bar{U}_{\bar{i}}} = \frac{k_j \sum_{i=a}^{b} V_i^{\mathrm{T}} C_j V_i}{\sum_{i=a}^{b} V_i^{\mathrm{T}} K V_i}, \tag{6}$$

where ${}_j\bar{U}_{\bar{i}}$ represents the average strain energy stored in the jth element. F_j will be denoted as the fractional mean strain energy of element j. Similarly, for the damaged structure:

$$F_j^* = \frac{{}_j\bar{U}_{\bar{i}}^*}{{}_s\bar{U}_{\bar{i}}^*} = \frac{k_j^* \sum_{i=a}^{b} V_i^{*\mathrm{T}} C_j V_i^*}{\sum_{i=a}^{b} V_i^{*\mathrm{T}} K^* V_i^*}. \tag{7}$$

The pre-damaged and the post-damaged fractional mean strain energy for jth element are related by

$$F_j^* = F_j + \mathrm{d}F_j, \tag{8}$$

where $\mathrm{d}F_j$ is related to the change in the fractional mean strain energy of the jth element resulting from the damage. The quantity $\mathrm{d}F_j$ can be obtained from the first order expansion [22]:

$$\mathrm{d}F_j \approx -F_j \alpha_j, \tag{9}$$

where the fractional change in stiffness, α_j, is given by

$$\alpha_j = \frac{\mathrm{d}k_j}{k_j} = \frac{k_j^* - k_j}{k_j}. \tag{10}$$

Define a damage index for the jth element as $\beta_j = k_j/k_j^*$. Then substituting Eqs. (6), (7), (9), and (10) into Eq. (8) and simplifying yields the damage index for the element j as

$$\beta_j = \frac{k_j}{k_j^*} = \frac{1}{2}\left(\frac{f_j^*}{f_j} + 1\right), \tag{11}$$

where the quantity f_j is given by

$$f_j = \frac{\sum_{i=a}^{b} V_i^{\mathrm{T}} C_j V_i}{\sum_{i=a}^{b} V_i^{\mathrm{T}} K V_i} \tag{12}$$

and

$$f_j^* = \frac{\sum_{i=a}^{b} V_i^{*\mathrm{T}} C_j V_i^*}{\sum_{i=a}^{b} V_i^{*\mathrm{T}} K^* V_i^*}. \tag{13}$$

Note that the damage index obtained using Eq. (11) is most susceptible to measurement and numerical errors when both numerator and denominator are close to zero. This phenomenon, for example, might be observed for elements near supports when the element size and the displacements are small. In such cases, localization errors may result. To avoid this problem, the domain of interest in the problem is shifted by adding unity to the denominator and numerator of Eq. (11) [22]. The resulting non-singular damage index is then given by the equation

$$\beta_j \approx \frac{\sum_{i=1}^{NT} V_i^{\mathrm{T}} K V_i}{\sum_{i=1}^{NT} V_i^{*\mathrm{T}} K V_i^*} \left(\frac{\sum_{i=1}^{NT} V_i^{*\mathrm{T}} C_j V_i^* + \sum_{i=1}^{NT} V_i^{*\mathrm{T}} K V_i^*}{\sum_{i=1}^{NT} V_i^{\mathrm{T}} C_j V_i + \sum_{i=1}^{NT} V_i^{\mathrm{T}} K V_i}\right). \tag{14}$$

Note that the damage index shown in Eq. (14) is the ratio of the effective stiffness of an element of the pre-damaged state to the post-damaged state.

2.2. Damage localization using the new damage ratio

Possible locations of damage in a structure can be identified by utilizing classification algorithms with the damage index given by Eq. (14) taken as the feature vector. As presented in a prior study [2], classification of an element as damaged or not damaged can be made on the basis of such schemes as (1) Bayes' rule (from which the well-known Linear and Quadratic Discriminant Analysis are derived) [23]; (2) nearest distance [24]; and (c) hypothesis testing [25]. In this study, hypothesis testing is used for the classification of an element as being damaged or not damaged. In hypothesis testing, the alternate hypothesis (H_1) and null hypothesis (H_0) are defined as H_0: element j of the structure is not damaged, H_1: element j of the structure is damaged.

To test the hypotheses, the damage indices shown in Eq. (14) are standardized using the equation

$$z_{ij} = \frac{\beta_{ij} - \mu_\beta}{\sigma_\beta}. \tag{15}$$

Here, it is assumed that the damage index, β_{ij}, is a random variable and the collection of the damage indices are distributed normally. Thus, a typical probability density function of the standardized damage indices for elements can be depicted as shown in Fig. 1. The one-tailed test to decide on the existence of damage in an element may be restated as (1) choose H_0 if $z_j < z_\eta$, (2) choose H_1 if $z_j \geqslant z_\eta$, where the quantity z_β is the standardized damage index, the quantity z_η is a threshold value of z_β, and η represents the level of significance of the test (see Fig. 1). The decision-making criterion for assigning the location of damage is thus established using elements of statistical decision-making. One can choose a greater threshold value to have more confidence in the identified damage locations. Note that a typical value for the level of significance in damage localization is 0.05 which corresponds to a z score of $z_{0.05} = 1.645$.

2.3. Severity estimation using the new damage ratio

Once the possible locations of damage are isolated, corresponding damage severities can be obtained using the corresponding damage indices to localized damage locations. Since the damage index is the ratio of pre-damage stiffness to post-damage stiffness, the severity of damage for jth

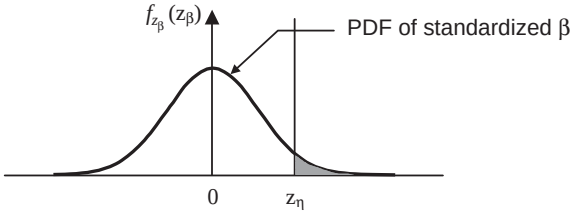

Fig. 1. Assumed probability density functions of standardized damage index.

element (i.e., the fractional loss in stiffness) may be expressed as

$$\alpha_j = \frac{k_j^* - k_j}{k_j} = \frac{1}{\beta_j} - 1. \tag{16}$$

Note that the severity of damage obtained using Eq. (16) represents the effective stiffness loss to undamaged stiffness for a specific element j of the structure.

3. Verification of methodology using simulated damage

The feasibility and performance of the proposed NDE algorithm is examined via a numerical example of a continuous beam structure. The example structure, shown in Fig. 2, is a three-span plate girder, and consists of two cross-sectional properties designated here as thick- and thin-flanged girder elements.

The sectional and material properties of the members of the structure are summarized in Table 1. Two-node cubic beam elements are used to model the example structure. The model has 60 elements and 61 nodes, as shown in Fig. 2. The structure is subjected to 15 damage scenarios. The locations and corresponding magnitudes of the damage simulated for each damage scenarios are summarized in Table 2. The damage is numerically simulated by reducing the elastic modulus of the appropriate elements. Forced vibration analysis was performed to compute time responses using a commercial FORTRAN code [26]. An impulse load is used to excite the structure at Node 31 in the vertical direction. The impact loading is shown in Fig. 3 and the location of the excitation is shown in Fig. 2. A direct integration method, the Newmark-β method [27], was used to generate the time response data. A magnitude of 0.1% viscous damping, which is typical for steel structures [28], was assumed for the structure. The displacement response data are assumed to be measured at 61 locations ($n = 61$) which correspond to the node points in Fig. 2. In real world applications using currently available technology, such a dense arrangement is not practical; however, the purpose of this paper is to establish the feasibility of the approach. The impact of using fewer sensors per span will be addressed in subsequent studies. Note that responses of the structure were sampled at each node for 2 s in time intervals of 0.002 s ($\Delta t = 0.002$) after the loading had been applied. Thus, a total of 1000 discrete displacement measurements ($NT = 1000$) were sampled for each node.

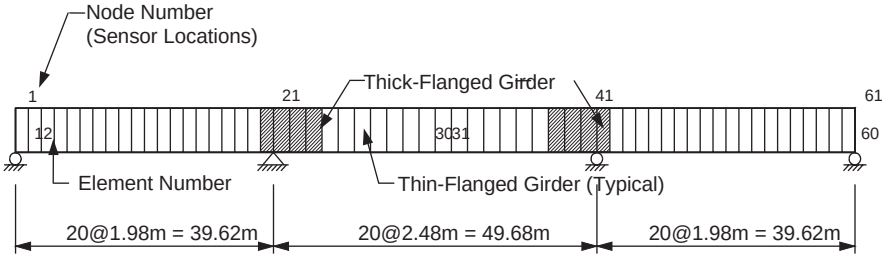

Fig. 2. Schematic of the finite element model of the continuous beam.

Table 1
Sectional and material properties of the beam structure

	Thick-flanged girder	Thin-flanged girder
Area (cm^2)	1103	697
Second moment of inertia (m^4)	0.2197	0.1193
Depth of the girder (cm)	305	305
Flange thickness (cm)	6.67	3.81
Flange width (cm)	61	53.34
Web thickness (cm)	0.95	0.95
Elastic modulus (GPa)	200	200
Mess density (kg/m^3)	7850	7850

Table 2
Simulated damage locations and severities

Damage scenario	Elements damaged			Corresponding severity (%)		
1	5			6.0		
2	32			16.0		
3	54			9.0		
4	20			3.0		
5	56			7.0		
6	15	10		7.0	9.0	
7	12	37		16.0	7.0	
8	7	21		3.0	5.0	
9	26	31		8.0	4.0	
10	3	42		4.0	2.0	
11	33	11	47	3.0	5.0	12.0
12	42	34	8	7.0	3.0	4.0
13	50	15	4	3.0	12.0	5.0
14	53	9	16	7.0	8.0	13.0
15	6	35	40	2.0	5.0	8.0

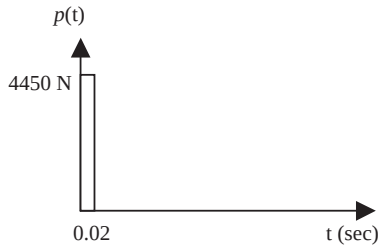

Fig. 3. Dynamic loading used to excite the continuous beam.

3.1. Measurement noise

In field application, it is expected that there would be some deviations due to measurement noise. In this example, the measurement noise is simulated by adding a series of random numbers

to the obtained mean strain energies for elements in the example structure. The random numbers are generated from a uniform distribution on the interval $[-1, 1]$. The degree of noise is determined by a noise/signal (NS) ratio that is a ratio of the random-number series to the amplitude of the mean strain energy [29]. In present applications, the effect of different level of noise on damage identification is investigated by applying 1% and 2% NS ratios.

3.2. Damage localization and severity estimation results

Using the damage index expression, presented in Eq. (14), the determination of the locations of potential damage in the structure is implemented using the following steps. First, the damage indices for each element are calculated using Eq. (14). Second, the obtained damage indices are standardized using Eq. (15). Third, the presence of damage in element j is determined according to the pre-assigned classification rules: (1) the element is damaged if $z_j \geqslant 2.0$; (2) the element is not damaged if $z_j < 2.0$. Note that the value of the damage indicator, 2.0, corresponds to a 0.02 level of significance test for the presence of damage.

The severity of damage is estimated using Eq. (16). The severity of damage for possible damage locations was estimated as follows. First, the possible damage elements are identified using the hypothesis testing algorithm. Second, the severity of damage is estimated using the damage indices for the possible damaged element using Eq. (16).

3.3. Results

The damage localization results are shown in Figs. 4–6. In all of the figures, note that the inflicted locations of damage are indicated by the tilted arrows near the horizontal axis. The vertical axis is in the non-dimensional units of the standardized damage ratios for that particular location. The percentage of false positives predictions (Type I error) and the percentage of false negatives predictions (Type II error) are used to evaluate the performance of the methodology. A false positive means that damage is reported where no damage exists and a false negative means that damage is not reported where damage exists. The percentage of false positives is calculated by dividing the number of false positive predictions by the number of undamaged elements, and the percentage of false negatives is calculated by dividing the number of false negative predictions by the number of damaged elements. The percent of false positives may reflect the quality of the measured data as well as the effectiveness of the damage localization algorithm while the percentage of false negatives may measure the sensitivity of measures to damage and the ability of the classification algorithm to correctly identify the damage location. The resulting percentage of false positives and negatives are summarized in Table 3.

For damage cases with a single damage location that correspond to damage cases 1–5, the proposed methodology successfully identifies all simulated damage locations (zero false negatives) with noise free data (see Fig. 4). Few false positives were observed but all the false positive predictions arise in the neighborhood of the simulated damage locations. When noise added, the methodology identified all damage locations except damage case 4 where the magnitude of the simulated damage was relatively small. As the NS ratio increased, it was observed that the standardized value for the damage index at a damage location was decreased.

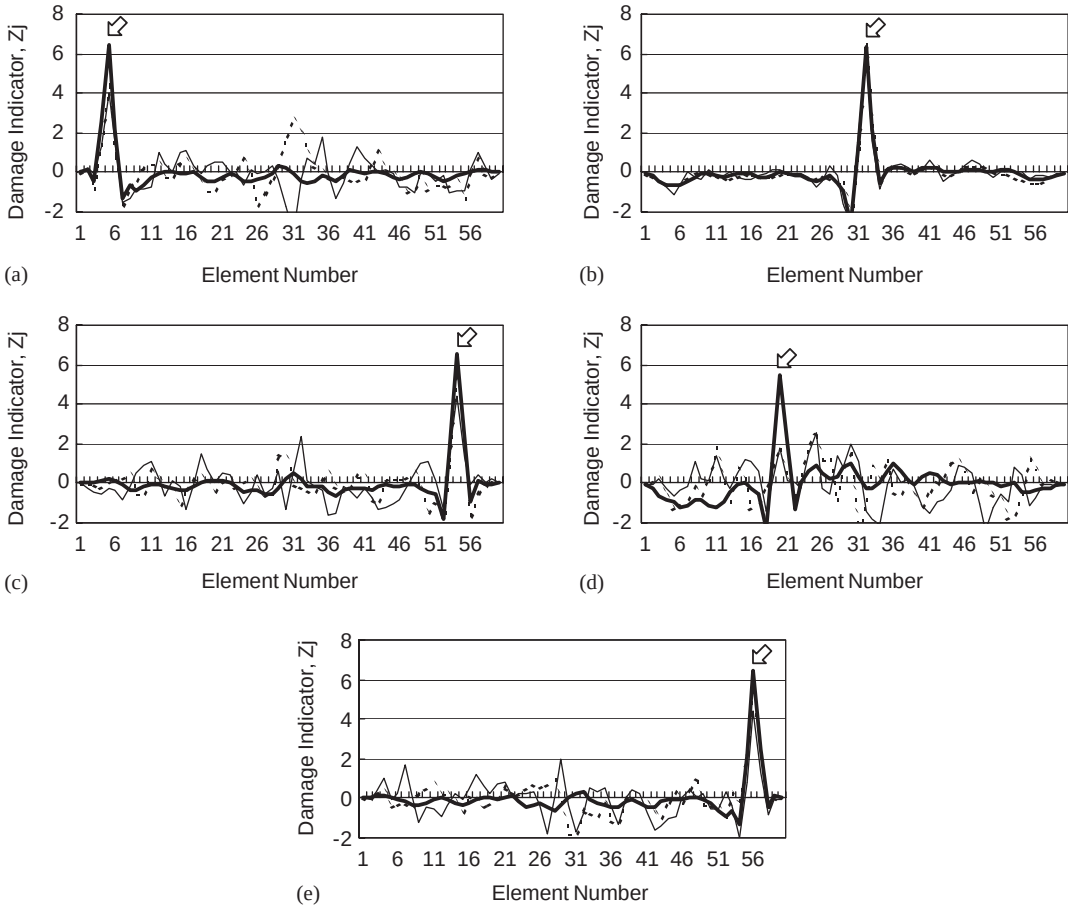

Fig. 4. Damage localization results for damage Cases 1–5: (a) damage case 1, (b) damage case 2, (c) damage case 3, (d) damage case 4, (e) damage case 5. ⇖ location of damage; ▬, noise free; - - - -, 1% NS; ——, 2% NS.

In the damage localization results for damage cases with multiple damage locations, damage cases 6–15, the proposed localization methodology performed quite satisfactorily with noise free data (see Figs. 5 and 6). In only two damage scenarios, damage case 13 and 15 in which the structure was damaged at 3 locations, the standardized value for the damage index was between 1 and 2. However, all three damage locations in those two damage cases can be inferred from Fig. 6. From a review of the damage magnitudes inflicted at the various locations and presented in Table 2, one explanation for the lower value of the standardized damage index in the latter cases is the possible masking of the smallest damage magnitudes at location 50 in damage case 13 and location 6 in damage case 15. When noise was added, it was observed that the percentage of false negatives was increased as the NS ratio increased. However, even with the severest simulated noise level when the NS ratio was 2%, most of damage locations can be inferred from Figs. 5 and 6. It can be seen in the figures that, with a lower significance level of the test (less confidence in the presence of damage), the detectability of the method can be improved dramatically. For example, when the NS ratio is 2%, with the threshold value of 1.5, the number of false negatives can be

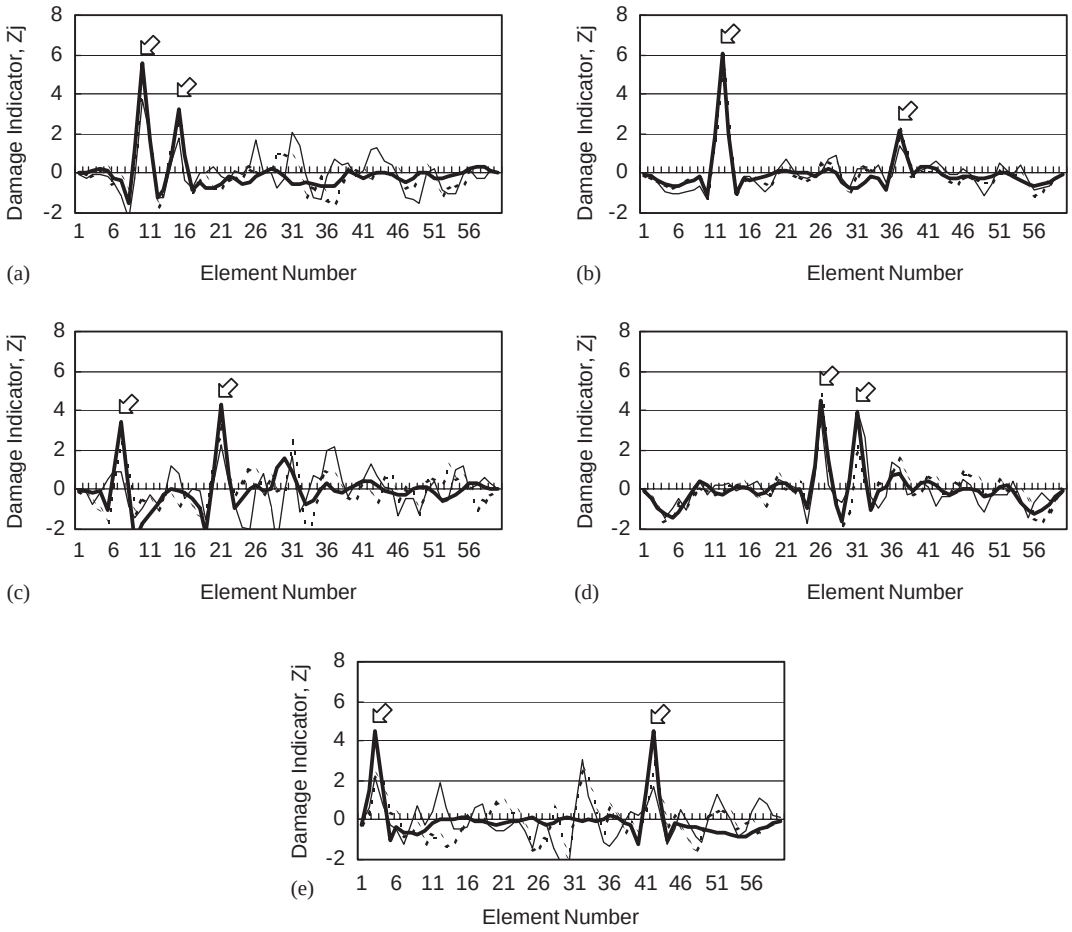

Fig. 5. Damage localization results for damage Cases 6–10: (a) damage case 6, (b) damage case 7, (c) damage case 8, (d) damage case 9, (e) damage case 10. ⇖ location of damage; ▬, noise free; - - - -, 1% NS; ——, 2% NS.

decreased to three from nine in all damage cases with multiple damage locations (Figs. 5 and 6). From Table 3, the percentage of false positives seemed not to be influenced significantly by the increased number of damage locations and the noise level. However, it can be inferred from the figures that the number of false positives will be increased with a lower significance level of the test.

Another way to evaluate the performance of the proposed method is as follows. In all 15 damage cases a total of 30 damage sites were inflicted. Without noise, the method unambiguously located 28 of these 30 cases. This result corresponds to an overall success rate of 93%. With additional screening of the data or lowering the significance level of the test, the success rate for the sample used here could be as high as 100%. When noise was added, the method identified 26 and 21 in 30 simulated damage locations, which corresponds a success rate of 87% and 70%, respectively.

The severity estimation results using the proposed methodology are presented in Table 4. For all damage cases, the proposed methodology consistently yields lower damage severity estimates

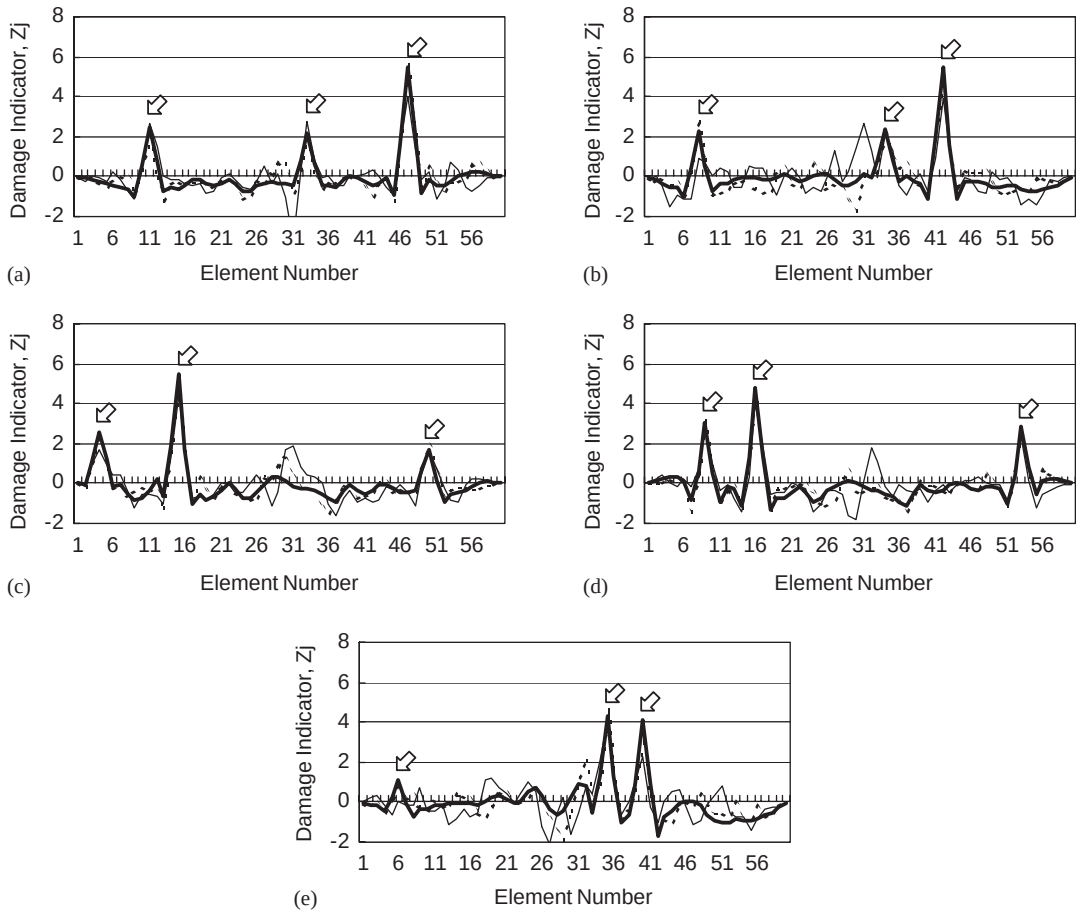

Fig. 6. Damage localization results for damage Cases 11–15: (a) damage case 11, (b) damage case 12, (c) damage case 13, (d) damage case 14, (e) damage case 15. ⇖ location of damage; ——, noise free; - - - -, 1% NS; ——, 2% NS.

than the simulated values. The fact that damage is smeared into the neighboring elements, as shown in Figs. 4–6, may explain this systematic error. In the table, it was also observed that the proposed methodology gives a reasonable agreement between damage magnitudes using the noise-free and the noise-polluted data.

4. Summary and conclusion

In this paper, a damage localization and severity estimation methodology using time-domain response data was presented. The motivation for the approach was to investigate the possibility of obviating certain drawbacks associated with commonly used modal extraction parameter methods. The time-domain displacement response measurements were assumed to be measured at a finite number of locations in a structure and the mean strain energy over a specified time interval was obtained for each and every element of the structure. The mean strain energy for the elements

Table 3
Number of false positives and false negatives

Damage case	False positives			False negatives		
	No noise	1% noise	2% noise	No noise	1% noise	2% noise
1	2 (3[a])	1 (2[a])	0 (0[a])	0 (0[b])	0 (0[b])	0 (0[b])
2	1 (2)	1 (2)	1 (2)	0 (0)	0 (0)	0 (0)
3	1 (2)	0 (0)	1 (2)	0 (0)	0 (0)	0 (0)
4	0 (0)	1 (2)	1 (2)	0 (0)	1 (100)	1 (100)
5	2 (3)	1 (2)	0 (0)	0 (0)	0 (0)	0 (0)
6	0 (0)	0 (0)	1 (2)	0 (0)	0 (0)	1 (50)
7	0 (0)	0 (0)	0 (0)	0 (0)	0 (0)	1 (50)
8	0 (0)	1 (2)	2 (3)	0 (0)	0 (0)	1 (50)
9	0 (0)	0 (0)	1 (2)	0 (0)	0 (0)	0 (0)
10	0 (0)	2 (3)	1 (2)	0 (0)	0 (0)	1 (50)
11	1 (2)	0 (0)	0 (0)	0 (0)	1 (33)	0 (0)
12	1 (2)	1 (2)	1 (2)	0 (0)	0 (0)	1 (67)
13	0 (0)	0 (0)	0 (0)	1 (33)	1 (33)	2 (33)
14	0 (0)	0 (0)	0 (0)	0 (0)	0 (0)	0 (0)
15	0 (0)	1 (2)	1 (2)	1 (33)	1 (33)	1 (33)
Σ	8 (1)	9 (1)	10 (1)	2 (7)	4 (13)	9 (30)

[a] Percentage of false positives.
[b] Percentage of false negatives.

was, in turn, used to build an element damage index defined as the ratio of the stiffness parameter of the pre-damaged to the post-damaged elements. The standardized damage indices were then used as feature vectors in a classification scheme to identify damage. Depending upon the value of the standardized damage index for a given element, the element was classified as either damaged or undamaged. The classification scheme used here was based on the statistical decision technique of hypothesis testing.

The feasibility of the methodology was demonstrated using simulated data from a continuous beam structure. The performance of the proposed methodology was evaluated in terms of the number of damage locations false-positive predictions, the number of false-negative predictions, and the accuracy of the damage severity predictions. A total of 15 damage cases were simulated. In these cases a total of thirty damage locations were simulated. Also, the robustness of the method to noise was investigated by adding the NS ratio of 1% and 2% to the noise-free data. With the same significance level of the test, the method correctly identified 93%, 87%, and 70% of the damage events using the noise-free, the 1% NS ratio, and the 2% NS ratio data, respectively.

From the numerical study, the following conclusions are drawn: (1) the time-domain response data may be used directly to localize and size damage in a structure; (2) the numerical simulation of a continuous beam reveals that the proposed methodology can identify single and multiple damage locations consistently and accurately even using the data with simulated noise; (3) the false negatives can be reduced using the lowered significance level of test for damage localization at the expense of increasing the number of false positives; and (4) the proposed methodology consistently produces lower damage severity estimations.

Table 4
Severity estimation results

Damage case	Element number	Simulated severity (%)	Estimated severity (%)		
			No noise	1% noise	2% noise
1	5	6.0	3.8	2.9	4.5
2	32	16.0	9.4	9.6	8.3
3	54	9.0	5.4	4.5	5.1
4	20	3.0	1.4	—	—
5	56	7.0	4.5	4.6	5.1
6	10	9.0	4.8	4.6	3.9
	15	7.0	3.8	3.7	—
7	12	16.0	9.9	9.5	10.4
	37	7.0	3.9	3.9	—
8	7	3.0	1.4	1.2	—
	21	5.0	2.7	2.6	3.3
9	26	8.0	4.4	4.3	4.4
	31	4.0	1.7	0.8	2.0
10	3	4.0	2.5	2.6	4.3
	42	2.0	1.1	1.5	1.5
11	11	5.0	2.8	—	4.0
	33	3.0	1.9	1.8	3.2
	47	12.0	7.5	7.6	7.3
12	8	4.0	1.9	2.7	—
	34	3.0	1.8	2.0	1.9
	42	7.0	4.2	3.2	3.7
13	4	5.0	3.8	3.6	—
	15	12.0	7.3	6.9	8.4
	50	3.0	—	—	—
14	9	8.0	3.7	3.8	4.3
	16	13.0	7.5	7.2	7.6
	53	7.0	3.5	3.3	3.5
15	6	2.0	—	—	—
	35	5.0	2.9	3.6	4.1
	40	8.0	4.6	4.2	3.9

References

[1] S.F. Masri, A.G. Chassiakos, T.K. Caughey, Identification of nonlinear dynamic systems using neural networks, *Journal of Applied Mechanics* 60 (1993) 123–133.
[2] N. Stubbs, G. Garcia, Application of pattern recognition to damage localization, *Microcomputers in Civil Engineering* 11 (1996) 395–409.
[3] N. Stubbs, R. Osegueda, Global non-destructive damage evaluation in solids, *The International Journal of Analytical and Experimental Modal Analysis* 5 (2) (1990) 67–79.
[4] N. Stubbs, R. Osegueda, Global damage detection in solids—experimental verification, *The International Journal of Analytical and Experimental Modal Analysis* 5 (2) (1990) 81–97.
[5] J.T.P. Yao, Damage assessment of existing structures, *Journal of Engineering Mechanics Division* 106 (4) (1980) 785–799.

[6] H.G. Natke, Updating computational models in the frequency domain based on measured data: a survey, *Probabilistic Engineering Mechanics* 8 (1988) 28–35.
[7] J.E. Mottershead, M.I. Friswell, Model updating in structural dynamics: a survey, *Journal of Sound and Vibration* 167 (1993) 347–375.
[8] N. Stubbs, J.T. Kim, K.G. Topole, An efficient and robust algorithm for damage localization in offshore platforms, *ASCE 10th Structures Congress'92*, 1992, pp. 543–546.
[9] C. Farrar, D. Jauregui, Damage detection algorithms applied to experimental and numerical modal data from the I-40 bridge, Technical Report LA-13074-MS, Los Alamos National Laboratory, 1996.
[10] P. Cawley, R.D. Adams, The location of defects in structures from measurements of natural frequencies, *Journal of Strain Analysis* 14 (2) (1979) 49–57.
[11] N. Stubbs, Non-destructive evaluation of damage in periodic structures, *Proceedings of the Third International Conference on Space Structures*, 1984, pp. 332–337.
[12] N. Stubbs, D. Rials, Non-destructive evaluation of damage in multi-story structure, *Structural Safety and Reliability* 2 (1985) 517–522.
[13] N. Stubbs, A general theory of non-destructive damage detection in structures, in: H.H.H. Leipholz (Ed.), *Structural Control*, 1985, pp. 694–713.
[14] S. Choi, N. Stubbs, Nondestructive damage detection algorithms for 2d plates, *Smart Structures and Materials 1997*: *Smart Systems for Bridges*, *Structures*, *and Highways*, *SPIE Proceedings*, Vol. 3043, 1997, pp. 193–204.
[15] J.T. Kim, N. Stubbs, Damage detection in offshore jacket structures from limited modal information, *International Journal of Offshore and Polar Engineering* 5 (1) (1995) 58–66.
[16] J.T. Kim, N. Stubbs, Model-uncertainty impact and damage-detection accuracy in plate girder, *Journal of Structural Engineering* 121 (10) (1995) 1409–1417.
[17] S. Park, N. Stubbs, R. Bolton, S. Choi, C. Sikorsky, Field verification of the damage index method in a concrete box-girder bridge via visual inspection, *Computer-Aided Civil and Infrastructure Engineering* 16 (2001) 58–70.
[18] D.J. Ewins, *Modal Testing: Theory and Practice*, Research Studies Press, Hertfordshire, England, 1986.
[19] M. Sanayei, O. Onipede, Damage assessment of structures using static test data, *American Institute of Aeronautics and Astronautics Journal* 29 (7) (1991) 1174–1179.
[20] M.S. Agbabian, S.F. Masri, R.K. Miller, T.K. Caughey, A system identification approach to the detection of structural changes, *Journal of the Engineering Mechanics* 117 (2) (1990) 370–390.
[21] B.C. Faulkner, F.W. Barton, T.T. Baber, W.T. Mckeel Jr., Determination of bridge response using acceleration data, Technical Report VTRC-97-R5, Virginia Transportation Research Council, 1996.
[22] S. Park, Development of a Methodology to Continuously Monitor the Safety of Complex Structures, PhD Dissertation, Texas A&M University, College Station, TX, 1997.
[23] J.D. Gibson, J.L. Melsa, *Introduction to Nonparametric Detection with Applications*, Academic Press, New York, 1975.
[24] M. Nadler, E.P. Smith, *Pattern Recognition Engineering*, Wiley, New York, 1993.
[25] R.L. Ott, *An Introduction to Statistical Methods and Data Analysis*, Wadsworth, Belmont, CA, 1993.
[26] ABAQUS, *Version 5.4 User's Manual*, Hibbitt, Karlsson & Sorensen Inc., Providence, RI, 1994.
[27] J.N. Reddy, *An Introduction to the Finite Element Method*, McGraw-Hill, New York, 1993.
[28] R.R. Craig, *Structural Dynamics—An Introduction to Computer Methods*, Wiley, New York, 1981.
[29] W.-X. Ren, G.D. Roeck, Structural damage identification using modal data I: simulation verification, *Journal of Structural Engineering* 128 (1) (2002) 87–95.